

PAPER • OPEN ACCESS

## Inhomogeneities and Extreme Fluctuations of Strains in Grains of Polycrystalline Materials

To cite this article: V E Shavshukov and A A Tashkinov 2019 *IOP Conf. Ser.: Mater. Sci. Eng.* **581** 012032

View the [article online](#) for updates and enhancements.

# Inhomogeneities and Extreme Fluctuations of Strains in Grains of Polycrystalline Materials

V E Shavshukov and A A Tashkinov

Perm National Research Polytechnic University, 29 Komsomolsky Av., Perm 614990, Russia

E-mail: shavshukov@pstu.ru

**Abstract.** Inhomogeneity of strains in individual grains are calculated using the field-theoretical approach in the mechanics of polycrystalline materials. It is shown that the microstructure surrounding the grain strongly influences the amplitude of the non-uniformity of strains in the grain. In the random microstructure of a polycrystal, there are specific clusters of grains in which very large strain fluctuations are realized. The strains in these clusters exceed macrostrains several times. The patterns of such extreme clusters are presented. Extreme strain fluctuations in bulk grains exceed fluctuations in surface grains by 40%. This may be one of the reasons for the movement of sites of damage initiation in gygacycle fatigue mode from the surface of a polycrystalline sample into the bulk.

## 1. Introduction

Determining microstructure-property relationships is an essential engineering problem and an important area of experimental and computational materials science. Due to the stochastic structure of polycrystals, the strain and stress fields at the meso-level are random, highly fluctuating inhomogeneous fields. Numerous studies described, for example, in review articles [1, 2, 3, 4], indicate the importance of estimating the magnitudes of strains fluctuations and their connection with the microstructure, especially in matters of gygacycle fatigue, where macro stresses and strains are very small. Fluctuations of strains in a grain depend on its shape, orientation, and interaction with the surrounding microstructure. Experiments of recent years using X-ray microscopy [5, 6, 7] revealed the existence of specific clusters of grains in polycrystals, which have a strong influence on the damage initiation and other localized critical phenomena. Extremely large strains and stresses are realized in these clusters. It was found that the interaction of grains plays a crucial role in the appearance of high strains and stresses [8, 9, 10].

Extreme clusters have characteristic microstructure patterns specific for different types of grain anisotropy and conditions of macro loading. The probability of the formation of these clusters is small; therefore, an experimental study of possible cluster patterns and extreme fluctuations of the fields in the cluster grains is difficult. As a result, the development of effective theoretical and computational tools for finding configurations of extreme clusters, estimating the magnitudes of fluctuations in random structures of polycrystals is relevant. In the present work, we carried out such estimates using the field-theoretical approach in the mechanics of polycrystals [11].



## 2. Field theory method for calculating strains in polycrystal grains

Let us consider a macroscopically isotropic polycrystalline body of volume  $V$ , surface  $S$ , and denote by,  $u_i(\vec{r})$ ,  $\varepsilon_{ij}(\vec{r})$ ,  $C_{ijkl}(\vec{r})$  the displacement vector, the strain tensor, and the elastic moduli tensor, respectively.

These variables are global fields. The elastic tensor is decomposed into homogenized and fluctuating parts

$$C_{ijkl}(\vec{r}) = \langle C_{ijkl} \rangle + C'_{ijkl}(\vec{r}), \quad (1)$$

where  $\langle C_{ijkl} \rangle \equiv \frac{1}{V} \int_V C_{ijkl}(\vec{r}) d\vec{r}$  is a homogeneous isotropic tensor, and  $C'_{ijkl}(\vec{r})$  - a rapidly oscillating tensor

function of arbitrary anisotropy and zero mean value. The isotropic tensor has the form

$$\langle C_{ijkl} \rangle = 3\langle K \rangle V_{ijkl} + 2\langle \mu \rangle D_{ijkl}, \quad (2)$$

where  $\langle K \rangle$  and  $\langle \mu \rangle$  are the homogenized bulk modulus and shear modulus,  $V_{ijkl}$  and  $D_{ijkl}$  are the spherical and deviatoric parts of the identity tensor  $I_{ijkl} = (\delta_{ik}\delta_{jl} + \delta_{il}\delta_{jk})/2$ , and  $\delta_{ik}$  is the Kronecker symbol.

We set two boundary problems for this body. The first problem is posed for a body with a uniform tensor of elastic moduli  $\langle C_{ijkl} \rangle$ . The second problem is set for the same body with an inhomogeneous tensor  $C_{ijkl}(\vec{r})$ . The boundary conditions for both bodies are the same. We use the integral form of boundary value problems in displacements.

The vector of displacements in a homogeneous body with an homogenized tensor is denoted as  $u_m^*(\vec{r})$ . The integral equation for the displacement vector in such a body has the form [12]

$$u_m^*(\vec{r}) = \int f_i(\vec{r}') G_{im}(\vec{r} - \vec{r}') d^3\vec{r}' + \oint_S \langle C_{ijkl} \rangle [u_{k,l}^*(\vec{r}') G_{im}(\vec{r} - \vec{r}') - u_i^*(\vec{r}') G_{km,l}(\vec{r} - \vec{r}')] dS'_j, \quad (3)$$

where  $f_i(\vec{r})$  is the vector of volume forces,  $G_{im}(\vec{r})$  is the Green's function of an isotropic medium with an averaged tensor of elastic moduli  $\langle C_{ijkl} \rangle$ , the index after the comma means differentiation by the corresponding coordinate.

The displacement vector for the second problem in an inhomogeneous body with a tensor of elastic moduli  $C_{ijkl}(\vec{r})$  is denoted by  $u_m(\vec{r})$ . It satisfies the integral equation, which is derived similarly to (2) and has the form [11]

$$u_m(\vec{r}) = \int [C'_{ijkl}(\vec{r}') u_{k,l}(\vec{r}')]_j G_{im}(\vec{r} - \vec{r}') d^3\vec{r}' + \int f_i(\vec{r}') G_{im}(\vec{r} - \vec{r}') d^3\vec{r}' + \oint_\Gamma \langle C_{ijkl} \rangle [u_{k,l}(\vec{r}') G_{im}(\vec{r} - \vec{r}') - u_i(\vec{r}') G_{km,l}(\vec{r} - \vec{r}')] dS'_j. \quad (4)$$

Differentiating (3) and (4) and subtracting one from the other, as a result we obtain the equation for the global strain tensor  $\varepsilon_{mn}(\vec{r})$

$$\varepsilon_{mn}(\vec{r}) = \varepsilon_{mn}^*(\vec{r}) + \int_V g_{mnij}(\vec{r} - \vec{r}') C'_{ijkl}(\vec{r}') \varepsilon_{kl}(\vec{r}') d^3\vec{r}', \quad (5)$$

where  $g_{mnij}(\vec{r}) = [(G_{im,nj}(\vec{r}) + G_{in,mj}(\vec{r}))]/2$  is the modified Green tensor. Equation (5) was obtained by many authors [13, 14, 15] and used in various aspects. It is similar to the Lippmann-Schwinger equation in quantum field theory [14]. We use equation (5) to calculate inhomogeneous strains in the grains. To do this, we discretize the equation. First, we decompose the global strain fields and the elastic modulus tensor into a sum of local variables in the grains using the shape functions  $\lambda_\xi(\vec{r})$  of the grains (equal to one inside the grain and zero outside it)

$$\varepsilon_{ij}(\vec{r}) = \sum_{\xi=1}^N \lambda_\xi(\vec{r}) \varepsilon_{ij}^{(\xi)}(\vec{r}) \quad \text{and} \quad C_{ijmn}(\vec{r}) = \sum_{\xi=1}^N \lambda_\xi(\vec{r}) C_{ijmn}^{(\xi)}(\vec{r}), \quad (6)$$

where  $N$  is the total number of grains in a polycrystal.

Substituting (6) into (5) leads to a system of interrelated integral equations for local fields in the grains

$$\varepsilon_{ij}^{(\xi)}(\vec{r}_\xi) = \varepsilon_{ij}^* + \int_{\omega_\xi} d\vec{r}'_\xi g_{ijkl}(\vec{r}_\xi - \vec{r}'_\xi) C_{klmn}^{(\xi)} \varepsilon_{mn}^{(\xi)}(\vec{r}'_\xi) + \sum_{\eta \neq \xi} \int_{\omega_\eta} d\vec{r}'_\eta g_{ijkl}(\vec{r}_\xi - \vec{r}'_\eta) C_{klmn}^{(\eta)} \varepsilon_{mn}^{(\eta)}(\vec{r}'_\eta) \quad (7)$$

The subscript of the radius vector  $\vec{r}_\xi$  indicates that it changes in the region  $\omega_\xi$  of the  $\xi$ -th grain.

Next, we divide each grain into a large number of small subgrains and decompose the strains in the grains into sums of strains in the subgrains  $\varepsilon_{ij}^{(\xi)(a)}(\vec{r})$  using the indicator functions of the subgrains  $\mu_a^\xi(\vec{r})$  in which the upper Greek index enumerates the grains and the lower Latin index enumerates the subgrains inside the grain

$$\varepsilon_{ij}^{(\xi)}(\vec{r}) = \sum_{a=1}^n \mu_a^\xi(\vec{r}_\xi) \varepsilon_{ij}^{(\xi)(a)}(\vec{r}) \quad (8)$$

This provides exact system of equations for  $\varepsilon_{ij}^{(\xi)(a)}(\vec{r}_a)$

$$\begin{aligned} \varepsilon_{ij}^{(a)(\xi)}(\vec{r}_a) = & \varepsilon_{ij}^* + \int_{\omega_a} d\vec{r}'_a g_{ijkl}(\vec{r}_a - \vec{r}'_a) C_{klmn}^{(\xi)} \varepsilon_{mn}^{(a)(\xi)}(\vec{r}'_a) + \\ & + \sum_{b \neq a} \int_{\omega_b} d\vec{r}'_b g_{ijkl}(\vec{r}_a - \vec{r}'_b) C_{klmn}^{(\xi)} \varepsilon_{mn}^{(b)(\xi)}(\vec{r}'_b) + \sum_{\eta \neq \xi} \sum_{e=1}^n \int_{\omega_e} d\vec{r}'_e g_{ijkl}(\vec{r}_a - \vec{r}'_e) C_{klmn}^{(\eta)} \varepsilon_{mn}^{(e)(\eta)}(\vec{r}'_e) \end{aligned} \quad (9)$$

where term related to  $a$ -th subgrain of  $\xi$ -th grain extracted from under the sum. To solve (9) we use perturbation theory. Let us consider both sums as perturbation and expand solution into series upon it

$$\varepsilon_{ij}^{(a,b,e)(\xi,\eta)}(\vec{r}) = \varepsilon_{ij}^{(0)(a,b,e)(\xi,\eta)}(\vec{r}) + \varepsilon_{ij}^{(1)(a,b,e)(\xi,\eta)}(\vec{r}) + \dots \quad (10)$$

Iterating of (9) gives equations for corrections of all orders of magnitudes

$$\begin{aligned} \varepsilon_{ij}^{(0)(a)(\xi)}(\vec{r}_a) - \int_{\omega_a} d\vec{r}'_a g_{ijkl}(\vec{r}_a - \vec{r}'_a) C_{klmn}^{(\xi)} \varepsilon_{mn}^{(0)(a)(\xi)}(\vec{r}'_a) = & \varepsilon_{ij}^* \\ \varepsilon_{ij}^{(1)(a)(\xi)}(\vec{r}_a) - \int_{\omega_a} d\vec{r}'_a g_{ijkl}(\vec{r}_a - \vec{r}'_a) C_{klmn}^{(\xi)} \varepsilon_{mn}^{(1)(a)(\xi)}(\vec{r}'_a) = & \sum_{b \neq a} \int_{\omega_b} d\vec{r}'_b g_{ijkl}(\vec{r}_a - \vec{r}'_b) C_{klmn}^{(\xi)} \varepsilon_{mn}^{(0)(b)(\xi)}(\vec{r}'_b) + \\ & + \sum_{\eta \neq \xi} \sum_{e=1}^n \int_{\omega_e} d\vec{r}'_e g_{ijkl}(\vec{r}_a - \vec{r}'_e) C_{klmn}^{(\eta)} \varepsilon_{mn}^{(0)(e)(\eta)}(\vec{r}'_e) \end{aligned} \quad (11)$$

..... and so on.

In the following we restrict solution by first order on perturbation and make last step of problem discretization. We will take strains be constant inside subgrain (due to it's small sizes) and varied by step-wise manner when go to adjacent subgrain. Then system of integral equations (11) transforms into system of linear algebraic ones

$$\begin{aligned} \varepsilon_{ij}^{(0)(a)(\xi)} - B_{ijkl}^{(aa)(\xi)} \varepsilon_{kl}^{(0)(a)(\xi)} = & \varepsilon_{ij}^* \\ \varepsilon_{ij}^{(1)(a)(\xi)} - B_{ijkl}^{(aa)(\xi)} \varepsilon_{mn}^{(1)(a)(\xi)} = & \sum_{b \neq a} B_{ijkl}^{(ab)(\xi)} \varepsilon_{kl}^{(0)(b)(\xi)} + \sum_{\eta \neq \xi} \sum_{e=1}^n B_{ijkl}^{(ae)(\eta)} \varepsilon_{kl}^{(0)(e)(\eta)}, \end{aligned} \quad (12)$$

where constant coefficients  $B_{ijmn}^{(ab)(\xi)} \equiv \int_{\omega_b} d\vec{r}'_b g_{ijkl}(\vec{r}_a - \vec{r}'_b) \cdot C_{klmn}^{(\xi)}$  and  $B_{ijmn}^{(ae)(\eta)} \equiv \int_{\omega_b} d\vec{r}'_b g_{ijkl}(\vec{r}_a - \vec{r}'_b) \cdot C_{klmn}^{(\eta)}$  describe

interactions of subgains inside the same grain and in different grains. These coefficients depend on microstructure of polycrystal and can be found numerically.

### 3. Numerical results for model polycrystals

We perform calculations on model polycrystals with spherical and cubic grains of equal volume. Consider a spherical  $\xi$ -th grain immersed in the averaged medium of all other polycrystal grains. In this case, as shown in [16], all corrections of higher order in exact equations (11) vanish, and corrections of zero order are the same for all subgrains of a spherical grain and are found from the algebraic equation

$$\left\{ I_{ijmn} + \frac{1}{3\langle\mu\rangle} \left[ (1-\chi)V_{ijkl} + \left(1 - \frac{2}{5}\chi\right)D_{ijkl} \right] \cdot C'_{klmn} \right\} \varepsilon_{mn}^{(a)} = \varepsilon_{ij}^*, \quad (13)$$

where  $\chi = (3\langle K \rangle + \langle \mu \rangle) / (3\langle K \rangle + 4\langle \mu \rangle)$ . For an isotropic grain in an isotropic matrix, the solution of (13) coincides with the Eshelby solution [17]. Inhomogeneity of strains in a spherical grain can occur only due to interaction with a non-uniform environment.

In a cubic single grain inside the inscribed sphere with a diameter of 0.9 from the cube edge, the strains are also almost homogeneous and coincide with strains in a spherical grain with an accuracy of several percent. Continuous singularities take place near the edges of the cube. The interaction with the inhomogeneous environment of the cubic grain makes the deformations inhomogeneous inside this spherical region. Numerical solution of equations (12) gives the deformation at any point of the grain under consideration, depending on the surrounding microstructure. In this model, this microstructure is reduced to the orientation of the crystallographic axes of each neighboring grain. An algorithm has been developed that searches for extremes of deformations at any point of the grain and the corresponding microstructures of the environment. The algorithm sets the array of random orientations of the surrounding grains, for each orientation solves system (12), from the array of solutions it finds the maximum (or minimum) value and the corresponding microstructure of the environment. Table 1 shows the results of calculations for a zinc polycrystal under uniaxial tension along the vertical axis  $X_3$ .

**Table 1.** Extreme deformation at grain points.

Macro strain $\varepsilon_{33}^* = 3 \cdot 10^{-4}$		Strain at given point $\varepsilon_{33}$
Grain center	maximum	$10.66 \cdot 10^{-4}$
	minimum	$-3.66 \cdot 10^{-4}$
Grain zenith	maximum	$11.34 \cdot 10^{-4}$
	minimum	$-2.79 \cdot 10^{-4}$

The absolute maximum is observed on the periphery of the grain at the zenith of the spherical part, the absolute minimum in the center of the grain. The maximum strain in the grain exceeds the macrostrain 3.78 times. The maximum (or minimum) strain at any point corresponds to a well-defined microstructure of the surrounding grains. Figure 1 shows a microstructure that generates a strain maximum in the center of the grain under consideration.

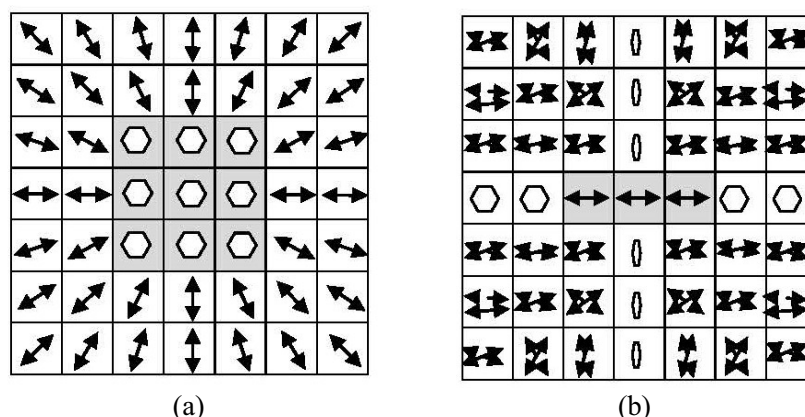


**Figure 1.** Extreme grain orientation of neighbors: horizontal (a) and vertical (b) section. Conventions in the text.

The hexagon conventionally depicts the plane of the hexagonal elastic symmetry of single crystal grains. The icon  corresponds to the position of the symmetry plane in the drawing plane, the icon

↔ depicts the position perpendicular to the drawing plane, and its inclination approximately shows the angle between the normal to the plane of elastic symmetry and the  $X_3$  axis, the icon  $\square$  corresponds to the inclined position to the drawing plane at some angle, but at the same time the normal of the plane of symmetry is perpendicular to the axis  $X_3$ . In an extreme configuration, clusters of grain-neighbors form symmetrical patterns. The nearest neighbors form a flat disk-shaped cluster of 9 grains of the same orientation around the central grain (they are darkened in Figure 1). The plane of the disk is perpendicular to the direction of the load. The tensile stiffness of these 9 grains is minimal in the direction of the load, while the surrounding grains are maximal. They form a kind of weakening zone. The diameter of this zone is equal to three grain diameters. If we introduce into the model a weakening zone of 5 grain diameters, then the strain in the central grain will decrease. It was experimentally found that in ultra-high cycle fatigue regime, cracks originate just in clusters of equally oriented grains [5], and the cluster size is equal to 3–4 grain diameters.

The magnitude of the fluctuations is significantly different for the bulk and surface grains of the polycrystal. The grain on the surface interacts with almost half as many neighbors as the grains deep inside the sample. As a result, the maximum possible strains in the surface grains are less by 40% compared to deep bulk grains. The range of fluctuations also decreases. Figure 2 shows the dependence of the maximum strain in the grain center on the distance from the surface of the sample. Thus, the surface grains form a special layer of material. In a sense, this is the discharge area of a polycrystalline body. The thickness of the surface layer is approximately equal to four average grain diameters.

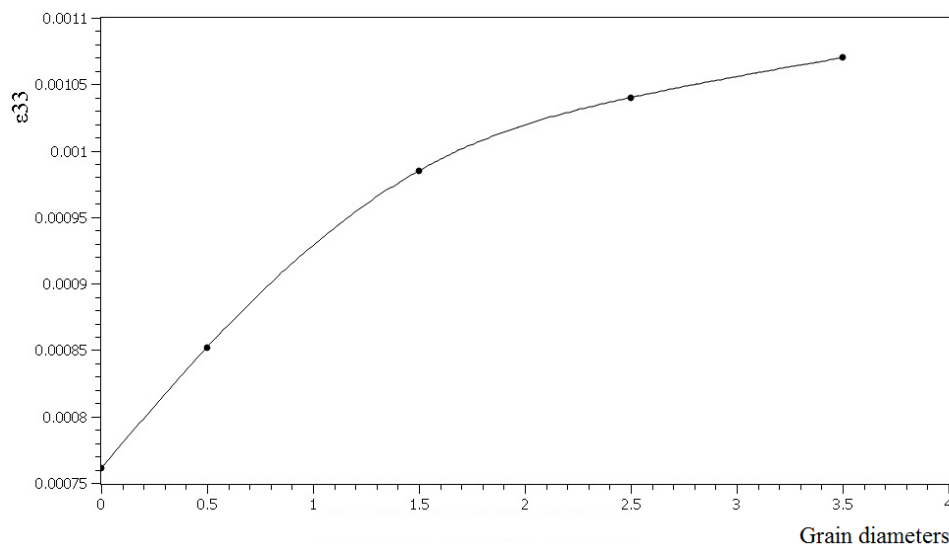


**Figure 2.** The dependence of the maximum strain on the distance to the surface.

#### 4. Conclusions

A characteristic feature of polycrystalline materials is a high degree of heterogeneity of kinematic and force fields in combination with a stochastic internal structure. This heterogeneity is insignificant in some cases, but it becomes crucial in the study of various critical phenomena, the occurrence of which strongly depends on the microstructure of the material. In this work, extreme strains in grains of polycrystals are investigated using the field theory approach. In a zinc polycrystal, the grains of which have a high anisotropy, the maximum strains in the grain are 3.78 times greater than the macrostrain. Such a concentration is due exclusively to the elastic interaction of structure inhomogeneities. Maximum deformations in deep bulk grains are 40% higher than in surface ones. This may be the cause of the movement of sites of damage initiations from the surface inside the samples during the transition from high-cycle to ultra-high-cycle fatigue.

The calculations were performed on model polycrystals with cubic grains. Calculations on polycrystals with a different grain shape give similar results. Against the background of the geometric symmetry of the models, patterns of extreme microstructure of the environment of the grains generating extreme deformations clearly manifest themselves. The specific type of patterns depends on the anisotropy of the grains and the type of loading. In particular, it is theoretically predicted that maximum deformations under uniaxial tension arise in the center of the cluster from the nearest neighbors with the same orientation, that is, in fact, a large grain of a specific shape and orientation.

### Acknowledgment

This work was supported by the Russian Foundation for Basic Research under grants 18-01-00675, 17-41-590433 and 19-41-590021.

### References

- [1] Pineau A, Benzerga A A, Pardoën T 2016 *Acta Materialia* **107** 424-483
- [2] Pineau A, McDowell D L, Busso E P, Antolovich S D 2016 *Acta Materialia* **107** 484-507
- [3] Das A. 2017 *Philosophical Magazine* **97** 867-916
- [4] Fullwood D T, Niezgodá S R, Adams B L, Kalidindi S R 2010 *Prog. Mater. Sci.* **55** 477-562
- [5] Oja M, Chandran K S and Tyron R J 2010 *Int. J. Fatigue* **32** 551-556
- [6] Zimmermann M 2012 *Int. Mater. Reviews* **57** 73-91
- [7] Davidson D L, Tryon R G, Oja M, Matthews R and RaviChandra K S 2007 *Met. Mat. Trans.* **38A** 2214-25
- [8] Abdolvand H, Wright J and Wilkinson A 2018 *Nature Communications* **9** 171
- [9] Schuren J C, et all 2015 *Current Opinion in Solid State and Materials Science* **19** 235-244
- [10] Guilhem Y, Basseville S, Gurtit F, Stephan J, Cailletaud G 2010 *Int. J. Fatigue* **32** 1748-76
- [11] Shavshukov V E 2018 *Physical Mesomechanics* **21** 67-75
- [12] deWit R 1960 *Solid State Physics* **10** 249-292
- [13] Dederichs P H and Zeller R 1973 *Z.Physik* **259** 103-116
- [14] Kroner E 1977 *J. Mech. Phys. Solids* **25** 137-155
- [15] Mura T 1987 *Micromechanics of Defects in Solids* (Martinus Nijhoff Publishers)
- [16] Tashkinov A A and Shavshukov V E 2018 *PNRPU Mechanics Bulletin* **1** 87-105
- [17] Eshelby J D 1957 *Proc. R. Soc. A* **241** 376-396